Journal of Cleaner Production 249 (2020) 119341

Contents lists available at ScienceDirect

Journal of Cleaner Production

journal homepage: www.elsevier.com/locate/jclepro

Development of water-resisting mortar by incorporation of functionalized waste incineration ashes

Z.Y. Qu [a, b], Q. Alam [b], F. Gauvin [b, *], T. Dezaire [b], H.J.H. Brouwers [a, b], F.Z. Wang [a, **]

[a] State Key Laboratory of Silicate Materials for Architectures, Wuhan University of Technology, Wuhan, 430070, PR China
[b] Department of the Built Environment, Eindhoven University of Technology, P.O. Box 513, 5600, MB, Eindhoven, The Netherlands

ARTICLE INFO

Article history:
Received 18 March 2019
Received in revised form
17 October 2019
Accepted 15 November 2019
Available online 18 November 2019

Handling Editor: CT Lee

Keywords:
Bottom ash
Hydrophobic
Mortar
Stearic acid

ABSTRACT

In this study, a method to prepare water-resisting mortars by incorporating hydrophobic incineration ashes is reported. Bottom ash is the by-products of municipal solid waste incineration with limited recycling options due to harmful contaminants. To decrease the environmental risk of bottom ash and provide an economical and green route to reuse it, a wet chemistry method is applied to prepare hydrophobic bottom ash and investigate its potential to improve transport properties of concrete. The functionalization of fine bottom ash (<0.125 μm) using stearic acid provides hydrophobic nature to the particles along with improved leaching properties. At an optimum addition of 4% stearic acid, the bottom ash present a water contact angle of 141° and can be classified as hydrophobic. The influence of functionalized bottom ash on the cement hydration, mechanical properties, water absorption and wetting property of the water resisting mortar is investigated. Results show that the up to 30% of the binder can be replaced by hydrophobic bottom ash as it decreases the capillary water absorption rate and chloride penetration depth by 57% and 65%, respectively. The samples containing hydrophobic bottom ash show better mechanical properties as compared to the samples made with untreated bottom ash. The environmental assessment shows that the mortars containing functionalized BA are environmentally friendly because of the dilution effect and immobilization potential of the hazardous material into the cementitious matrix. Results show that the proposed method is a facile and efficient way to change bottom ash into hydrophobic powders, which leads to more environmentally friendly water-resisting mortar.

1. Introduction

For concrete structures designed for harsh environments, durability is a key factor that influences their reliability and safety (Hossain et al., 2016). In particular, ingress of water into the concrete is the most often occurring phenomenon that leads to the deterioration of concrete (Zhang et al., 2018). The ingress of water causes distress and provide passage to the aggressive ions such as Cl^- to reach inside the cementitious matrices (Elfmarkova et al., 2015), increasing the corrosion of steel reinforcement (Qu et al., 2018) and internal cracking due to the alkali-silica reaction (ASR). With a concern of global CO_2 output (cement industry itself estimated that cement production is responsible for 5% of the global CO_2 output), production of cement with recycled materials such as blast furnace slag could result in the decrease of CO_2 emissions (Carvalho et al., 2018). Taking the high maintenance and repair costs of concrete structures into account, it is significant to improve concrete durability sustainably and cleanly (Kalla et al., 2015). The most commonly used strategies to increase the water-resistance of concrete can be to increase the packing density (Ghafari et al., 2015), create tortuosity inside the system (Supit and Shaikh, 2015), improve the overall microstructure (Yang et al., 2018), limit the crack width (Van Tittelboom et al., 2010) and to use surface protection technologies (Liu and Hansen, 2016). However, even with these solutions, water ingress is challenging to eliminate due to the porous and micro-cracked structure of concrete (Wong et al., 2015).

Addition of hydrophobic materials to the system is an efficient way to prevent water penetration (Feng et al., 2002). The most frequently applied methods are either by surface treatments (Jiang et al., 2004) or by integrating hydrophobic components (Pham and Dickerson, 2014) into the bulk volume of the material. As

* Corresponding author.
** Corresponding author.
E-mail addresses: f.gauvin@tue.nl (F. Gauvin), fzhwang@whut.edu.cn (F.Z. Wang).

https://doi.org/10.1016/j.jclepro.2019.119341
0959-6526/

cementitious materials are vulnerable to the threat of microcracks, the bulk hydrophobic modification is an ideal way to increase the water-resistance of concrete (Wong et al., 2015). Silane-based repellents (Zhang et al., 2017) are widely used in concrete because of their versatility and easy dispersion in the water at room temperature (Shi et al., 2017). However, silanes are expensive (Qu and Yu, 2018) and poor wear resistance, which limits its large scale application in the concrete industry (De Vries and Polder, 1997). Another efficient way to prepare water resistance concrete is to add pretreated hydrophobic materials in the matrix. Wong et al. (2015) have prepared hydrophobic concrete with the addition of superhydrophobic paper sludge ash, which was modified by stearic acid through a physical ball milling method. This application shows that waste materials that are hard to recycle due to the presence of leachable heavy metals and salts can be used after functionalization (Silva et al., 2017).

Among the available waste materials, the fine fraction (<125 μm) of the Municipal solid waste incineration (MSWI) bottom ash (BA) is a good candidate, especially because these fines are usually highly contaminated with heavy metals, chlorides and sulfates (Alam et al., 2019c). Due to the high level of contaminants and low reactivity, BA finds little applications in the field of building materials and needs to be landfilled. With the increasing concern of environmental protection and stricter limitations for the leaching of contaminants from the landfilled materials, BA is encouraged to be reused as a secondary building material (Caprai et al., 2018b, 2018a). According to the recent Dutch initiative "Green Deal B-76", 100% of all BA produced in the Netherlands must be upgraded to a primary building material level before 2020 (Green deal-GD076, 2012). However, traditional treatments methods, such as sieving and washing (Alam et al., 2020), are unable to reduce the content of contaminants below the legal limits sets by the Dutch Soil Quality Decree (2007). Functionalization of these fines in order to modify their surface properties and to limit the leaching of contaminants can be used before the reuse in concrete.

The present research aims to investigate the feasibility of applying functionalized waste material to prepared water-resisting mortars. With a wet chemistry method, bottom ash is transferred into a hydrophobic powder, which presents potential to improve the transport property of cementitious materials. The influences of BA and hydrophobic bottom ash (HBA) to the cement hydration and mechanical properties of the mixed mortars are investigated. The transport property of the functionalized waste powder contained mortar was evaluated by water absorption and chloride penetration depth compared to the untreated waste powder contained mortar. The leaching behaviour of the BA, HBA and the mixed mortars are studied to assess the environmental impact of the water-resisting mortars. This work provides a facile and low-cost way to turn the fine fraction of BA into hydrophobic powders while decreasing the leaching of contaminants. This study also aims to provide an alternative recycling solution for BA by applying it into the mortar in order to increase its permeability.

2. Experiment

2.1. Materials

BA ≤ 4 mm used in this study was provided by Heros Sluiskil, the Netherlands. The fraction had already undergone a standard drying pre-treatment, including screening and removal of unburnt materials (Alam et al., 2017). The received BA was sieved to separate particles smaller than 125 μm with a vibratory sieve shaker (AS 450 Basic, Retsch, Germany) by DIN EN 933-1. The stearic acid (95%) was purchased from Sigma-Aldrich. The cement used in this study is Portland Cement CEM I 52.5 R, provided by ENCI (the Netherlands). Normal sand with the fraction ≤2 mm is used as aggregates (Graniet-Import Benelux, the Netherlands).

2.2. Preparation of the HBA

During the preparation of HBA, BA was dispersed in water under constant stirring. Then, different amounts of stearic acid (1%, 2%, 4%, 8%, 10% by weight of BA) are added to investigate the optimum content. After the reaction, the bottom ash was separated from the reaction mixture by filtration and dried overnight at 60 °C.

2.3. Testing methods

2.3.1. Characterization of the bottom ash

Morphology of the BA was characterized by a Phenom ProX scanning electron microscope (SEM) (Thermofisher Scientific, USA), with backscattered electron (BSE) detector at an accelerating voltage of 10 kV. All samples were sputtered-coated with a gold layer of approximately 15 nm in thickness.

The chemical composition of the BA was measured with the X-ray fluorescence spectrometer (XRF) (Omnian method: standardless) by using a PANalytical Epsilon 3 (Malvern Panalytical, the Netherlands). The sample for XRF was ignited at 1000 °C to measure the loss on ignition (LOI). Subsequently, the residues obtained after LOI were used to make glassy fused beads with fluxer oven (classisse leNeo).

The diffraction pattern was collected with a D2 X-ray diffractometer (XRD) (Bruker, USA). The XRD radiation source was Co; divergence slits 0.2° and soller slits of 2.5°. For the determination of amorphous content 10 wt% of Si was added as an internal standard. The Rietveld refinement was performed with TOPAS 4.2 (Bruker, USA) for the quantification of phases.

The FT-IR spectra of the original and hydrophobic BA were measured from 4000 to 400 cm^{-1} with a resolution of 4 cm^{-1} using a Frontier spectrometer (PerkinElmer, USA).

2.3.2. Characterization of the HBA

Hydrophobic bottom ash was characterized by various analytical methods. In order to measure the content of functionalizing agent (Stearic acid) associated with BA, thermogravimetric analyses (TGA) were performed on a STA 449 Jupiter® F1 400 System (Netzsch, USA), in a temperature range of 45–600 °C at a heating rate of 2 °C/min, under a nitrogen flow of 50 ml/min. This system was coupled to a Bruker Alpha Fourier transform infrared spectrometer to analyse the released vapours during the measurement.

The outlet gas flow was also captured in gas sorption tubes at the desorption temperatures, as characterized with the TGA-FTIR. The Gas tubes were then thermally desorbed with a TurboMatrix 350 Thermal Desorber (PerkinElmer, USA) and analysed with a Clarus 680 Gas Chromatograph and Clarus SQ 8 T Mass Spectrometer (GC-MS) (PerkinElmer, USA) according to the following temperature program, step 1: hold 50 °C for 6 min, elevate to 55 °C at 0.5 °C/min, hold 2 min at 55 °C, elevate to 300 °C at 20 °C, hold 4.75 min at 300 °C.

2.3.3. Preparation of the mortar samples

All mortar specimens were prepared in a laboratory mixer. The mortar was prepared with water: cement: sand = 0.5 : 1: 3 ratio. The replacement dosage of the BA and HBA is 10%, 20% and 30%. Firstly, the cement and water were added into the mixer followed by mixing for 1 min at lower speed and afterward it was mixed at medium speed for 120 s. The interval between both mixing steps was 30 s. Then, sand was added and mixed for another 120 s. The fresh mortar was then poured into plastic molds of $40 \times 40 \times 40$ mm^3 and vibrated for 1 min and covered with a plastic

film on the top surface for 24 h. All specimens were demolded and cured at a temperature of 20 °C and relative humidity of about 95% until their testing age. The dispersion of the HBA in the matrix was characterized by energy-dispersive X-ray spectroscopy (EDX) coupled with SEM, at high voltage (15 kV). A mapping of the mortar surface is made by using carbon as a target element.

2.3.4. Characterization of the mortar samples

The influence of the BA and HBA on the cement hydration kinetics was assessed by employing a TAM Air isothermal calorimeter. The tests were carried out for 80 h at 20 °C. The results were normalized by the mass of solid powders. The compressive strengths of the specimens were tested at the age of 7, 14 and 28 days, according to EN 196-1 (EN, 2005). The capillary water absorption of the mortar was determined according to EN 480-5. The experiments started by storing the samples vertically in a chamber with an RH of about 65 ± 5% at room temperature (20 ± 1 °C) after curing the samples for 28 days. The samples were exposed to water with an immersion depth of about 3 mm for 43 days and the mass of the samples was periodically measured during the experiment. The 90 days' chloride penetration depth test was carried out to the samples at the curing age of 28 days, according to NT Build 443 (Build, 1995). To determine the water contact angle of the mortar, a piece of the plate-shaped specimen with a diameter of 5 cm is used.

2.3.5. Leaching analysis

BA, HBA and the crushed mortar samples are sieved below 4 mm and used for the leaching test in accordance with EN12457-2. Leachates were obtained by shaking a mixture of 6 g samples and 60 g distilled water (L/S ratio 10), for 24 h in a horizontally placed, sealed PE bottle on a linear reciprocating shaking device (Stuart SSL2). Subsequently, leachates were filtered and diluted five times in a 25 ml volumetric flask. The leachates were acidified with 50 μl 65 wt% ultrapure HNO_3 solution to prevent precipitation and filtered again. The contents of heavy metals in the leachates were determined by inductively coupled plasma-optical emission spectroscopy (ICP-OES; Varian 730-ES, USA).

Furthermore, the concentrations of sulfates and chlorides in the leachates were determined by ion chromatography (IC) (Dionex 1100, Thermofisher, USA) equipped with an ion-exchange column AS9-HS (2 × 250 mm). The results were compared to the limited leaching values based on the Dutch legislation (Soil Quality Decree, 2013).

3. Results and discussion

3.1. Characterization and modification of the waste material

The bottom ash fraction with the size fraction below 125 μm was selected for the hydrophobic functionalization because of the high level of contaminants (Alam et al., 2017). The morphology of the particles plays an important role concerning surface functionalization. In Fig. 1. SEM shows the random shape and size of the BA particles. The morphology of the particle leads to the heterogeneous surface characteristics and type of reactive groups, such as hydroxyl group, that adds the complexity for the surface modification.

3.1.1. Composition of BA

BA has a complex and heterogeneous chemical composition, as the elemental analysis shows in Table 1. The major oxides that account for more than 63 wt% are CaO, SiO_2, Al_2O_3 and Fe_2O_3. Moreover, BA also contains many heavy metals (Sb, Mn, Cu, Cr, Ni, Zn, Sr) that are considered as contaminants and strictly regulated via the Dutch environmental legislation (Soil Quality Decree, 2013).

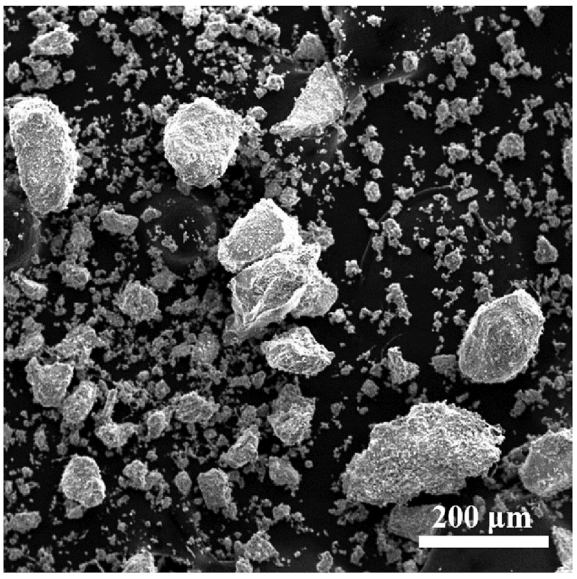

Fig. 1. The morphology of the fine BA particle with the size below 125 μm.

The potential leaching of these elements in the environment is the main factor that restricts the recycling applications of this material.

The understanding of the heterogeneous and complex mineralogy of the BA is required for the successful surface modification. The mineral composition of the BA is given in Table 2, which was determined with the quantitative XRD by using Rietveld analysis. The total crystalline content of the BA was 48 wt % and the rest consisted of the amorphous phases that cannot be distinguished from the diffraction pattern. The most abundant mineral in the BA was calcium carbonate ($CaCO_3$), also known as calcite, and its content was 20 wt%. In addition to that, other crystalline phases include silicates (quartz, melilite and feldspar) (Alam et al., 2019a), metallic oxides (spinel, hematite, lepidocrocite and rutile), sulfate-containing minerals (ettringite and gypsum) and the rest (apatite, zeolite and halite) (Alam et al., 2019b).

3.1.2. Optimal synthesis condition and characterization of the HBA

The optimum amount of stearic acid in the preparation of HBA is investigated, as shown in Fig. 2. With an increase from 1% to 4% addition amount of stearic acid, the water contact angle also increases from 76° to 141°. Then, the hydrophobicity of the HBA remains steady with the further addition of SA. In this study, the hydrophobic bottom ash (HBA) is prepared with 4% stearic acid for the application in a water-resisting mortar.

FTIR analyses of reference BA and HBA samples are presented in Fig. 3. It can be seen that the amount of SA has a significant impact on the FTIR spectra. Indeed, increasing the weight fraction of SA increase the intensity of various peaks, notably at 2914 and 2850 cm^{-1} or also 1575 cm^{-1}. In these FTIR patterns, all samples show a significant band at around 1480 cm^{-1}, which belong to the anti-symmetrical carboxylate ion ($-CO^{2-}$) stretching vibration and is associated with calcium carboxylate bonding. Only HBA exhibit absorption at 2914 cm^{-1} and 2850 cm^{-1}, which belong to the C—H stretch vibrations from the stearic acid. The intensity of these two peaks increases when more SA is added (Arbatan et al., 2011; Hu et al., 2009; Spathi et al., 2015). The absorption band at 1575 cm^{-1} is also only present in the HBA spectra and increases with the addition of stearic acid. This peak corresponds to anti-symmetrical carboxylate ion ($-CO_2-$) stretching vibration and can be associated with calcium carboxylate bonding. Moreover, HBA spectra show a unique absorption peak at 1588 cm^{-1},

Table 1
The chemical composition of BA obtained with XRF analysis (wt.%). R.O.: remaining oxides and LOI: loss on ignition measured at 1000 °C.

	CaO	SiO_2	Al_2O_3	Fe_2O_3	SO_3	MgO	P_2O_5	TiO_2	ZnO	K_2O	Sb_2O_3	MnO	CuO	R.O.	LOI
BA	25.0	19.6	12.6	6.3	3.7	1.7	1.6	1.4	0.8	0.5	0.3	0.2	0.2	0.3	25.8

Table 2
The mineral composition of the BA (wt.%) determined with the quantitative XRD using Rietveld analysis.

Minerals	BA
Calcite	20.3
Quartz	6.8
Apatite	4.7
Spinel	2.6
Ettringite	2.5
Gypsum	2.2
Melilite	2.1
Hematite	2.0
Feldspar	1.6
Zeolite	1.6
Lepidocrocite	0.8
Halite	0.7
Rutile	0.3
Amorphous	51.9

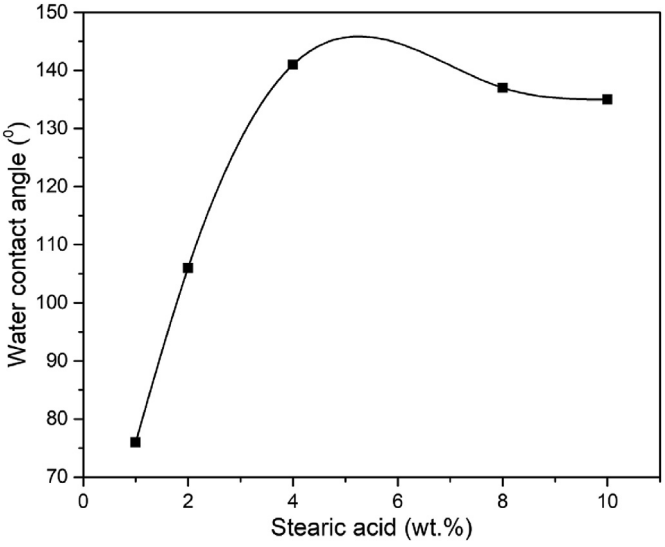

Fig. 2. The water contact angle of the HBA with the different stearic acid addition amounts (ranging from 1 to 10 wt%).

indicating that Ca^{2+} ions present at the surface reacted with the carboxyl groups of stearic acid, forming a layer of calcium stearate salt (Feng et al., 2018; Spathi et al., 2015). This method through wet chemistry route, can help to achieve chemical bonds between the SA and the BA, which would be useful for the long-term durability of the system.

The TGA coupled with FTIR analysis of the HBA is presented in Fig. 4. Negative peaks are artifacts due to the background analysis, which could not be eliminated with this method. Nonetheless, an intense absorption peak is visible at a temperature range of 360 and 450 °C. This peak consists of 2 peaks that are very close to each other between 2900 and 3000 cm^{-1}, which are characterized as C–H stretch vibrations in the hydrophobic tail of stearic acid, as seen in Fig. 4. These C–H stretch absorption bands are coming from the thermal decomposition of SA. The absence of carbonyl peak

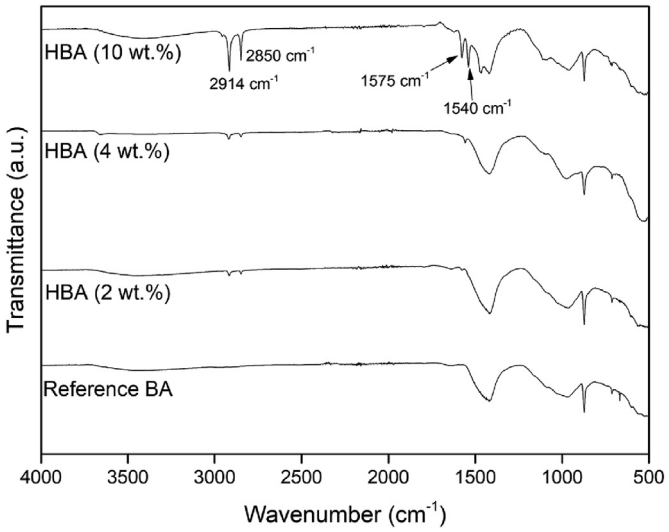

Fig. 3. FTIR spectra of the reference BA and the functionalized HBA with different wt.% of stearic acid.

around 1700 cm^{-1} can be explained by the very large amount of C–H bonds in stearic acid as compared to the other functions, but it can also mean that at this temperature, only short-chain hydrocarbon chains evaporate, indicating that the stearic acid is chemisorbed. Further characterization with GC-MS aims to elucidate this hypothesis.

Vapours are collected at 420 °C to be in the range characterized by TGA-FTIR showing the thermal degradation of the SA. The gas chromatogram is given in Fig. A1 (Appendix A), and the peaks are characterized by mass spectrum (MS) and their corresponding compounds are shown in Table 3. Most compounds are decomposition products of the C-18 hydrocarbon chain of the SA. It means that at a temperature above 360 °C, SA is still bonded to the BA, as characterized by TGA-FTIR and start to be fragmented by pyrolysis (Bolokang et al., 2015). This would indicate the chemisorption of the SA with BA, validating the proposed mechanism.

3.2. Processing and characterization of the water-resisting concrete

The HBA is mixed directly into the cement paste. As reported by (Du et al., 2015; Sanchez and Sobolev, 2010), the cluster of the functionalized powders is the key factor to influence the property of the hybrid concrete. SEM/EDX are used in order to characterize the dispersion of the HBA in the concrete, as shown in Fig. 5. Red pixels show the carbon element scattered in a 300 × 300 μm area. The analysis shows carbon concentrated at the surface, which appears to be HBA, with a particle size of 35–40 μm. It indicates that HBA is not agglomerated and well dispersed in the matrix.

3.2.1. Influence of BA and HBA on the cement hydration

The normalized heat flow and release of cement with different dosages of bottom ash replacement are shown in Fig. 6(a) and (b). It can be seen that the main heat release peak of the different samples is located at around 11.5 h. With the increase of the replacement dosage of bottom ash, the peak density is decreased. For the sample

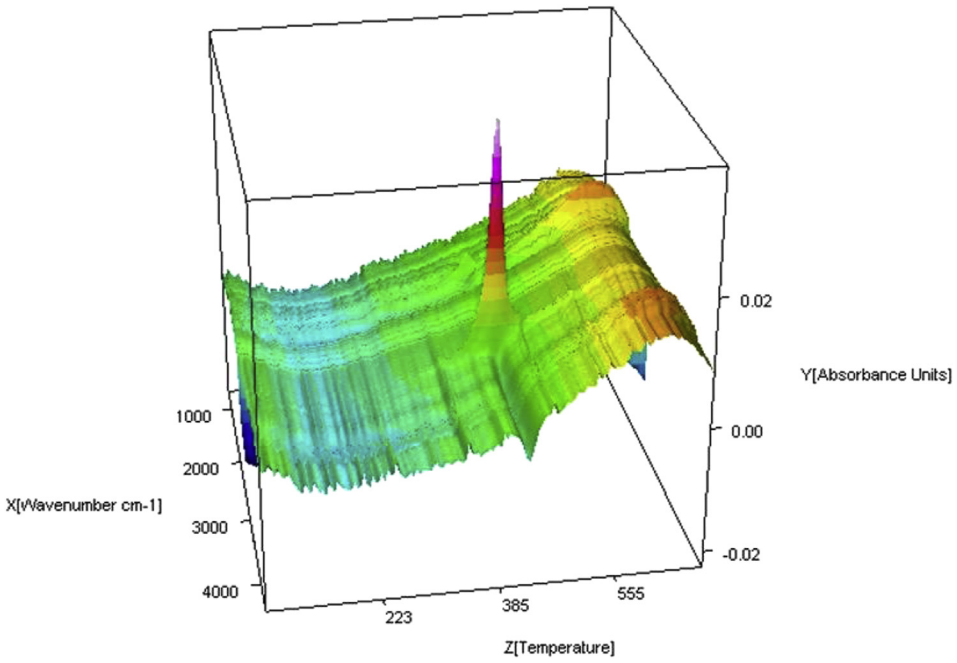

Fig. 4. 3D-spectrum of the TGA-FTIR measurement of the HBA (with 10 wt% of SA). Temperatures are in °C.

Table 3
Mass spectra library search results of the most important peaks in GC.

Retention time (min)	Compound name	Retention time (min)	Compound name
6.005	2-pentene	24.468	1-nonene
6.165	pentane	24.628	nonane
8.871	1-hexene	26.063	1-decene
9.246	hexane	26.173	decane
13.163	1,5-hexadiyne	27.219	1-undecene
15.329	1-heptene	27.294	undecane
16.139	heptane	28.149	1-dodecene
21.121	1,3,5-cycloheptatriene	28.214	dodecane
21.881	1-octene	28.959	1-tridecene
22.172	octane	29.014	tridecane
24.403	2-heptanone		

without BA, the peak density is around 4.5 mW/g while with 30% BA replacement, the peak density decreased to 3.2 mW/g. This is because that the BA works as non-reactive phases during the cement hydration (Caprai et al., 2018a). It should be noted that at the same dosages, the influence of both the BA and HBA to the hydration of cement is almost the same. This is also in line with the cumulative heat evolution, as shown in Fig. 6(b). The total heat release of the BA and HBA at the same replacement level is almost the same. This phenomenon illustrates that the stearic acid coating did not change the reaction kinetics of the cement, which also acts as a kind of non-reactive phase.

3.2.2. Mechanical property of the mortar

The effect of the BA and HBA on the compressive strength of the mixed mortar is shown in Fig. 7. The compressive strength of the reference samples is 36.8 MPa at 7 d. Then, it increases to 40.3 and 46.5 MPa at 14 d and 28 d, respectively. When replaced with bottom ash, the compressive strength of the mortar decreases continuously with different addition dosages. For the 30% replacement, the compressive strength decreases to 17.5 MPa, 20.6 MPa and 24.9 MPa at 7, 14 and 28 days. The obvious decrease of the mechanical property can be attributed to the porous structure of the BA after incineration, which results in lower strength of this powder (Gao et al., 2017). It should be noted that at the same age, the mortars containing HBA presents a higher compressive strength than the mortars containing BA. This can be attributed to the hydrophobic coating on the BA. With the hydrophobic coating of stearic acid, the water absorption of BA is limited. More water can be involved in cement hydration. Moreover, more water can enhance the homogeneous distribution of the paste in the molds resulting in good mechanical performance (Qu and Yu, 2018).

3.2.3. Transport property of the mortar

The results of capillary water absorption for 43 days and chloride penetration depth for 90 days are shown in Fig. 8 (a) and (b). With the addition of the HBA, the capillary water absorption of the mortar is decreased. For the reference sample, the water absorption at 28 days is 7.7% by weight mass and with 20% HBA and 30% HBA addition, the water absorption decreases to 5.1% and 3.3% at 28 days. The addition of hydrophobic agent results in water repellent lining among the pore structure in concrete (Liu and Hansen, 2016). These results are in line with the water contact angle results of the mortar, as shown in Fig. 9. The water contact angle of the mortar contained 10% HBA is 20.5° and increases up to 68.5° when the weight fraction increases to 30%. It should be noted that the addition of the untreated BA increases the water absorption of the mixed samples. At

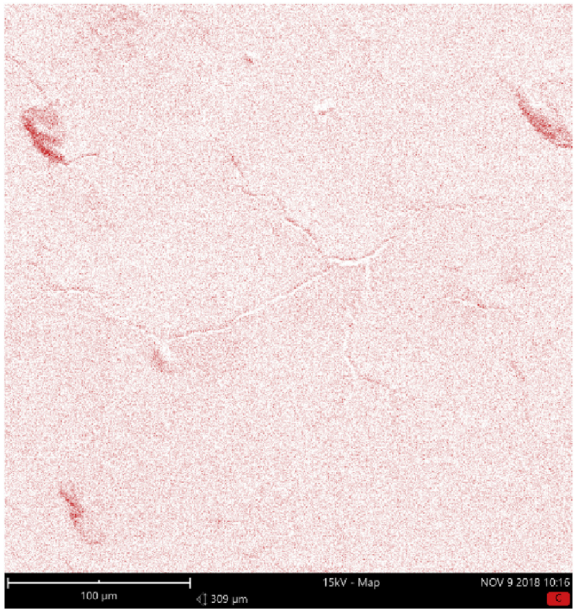

Fig. 5. The distribution of HBA in the water-resisting concrete by EDX.

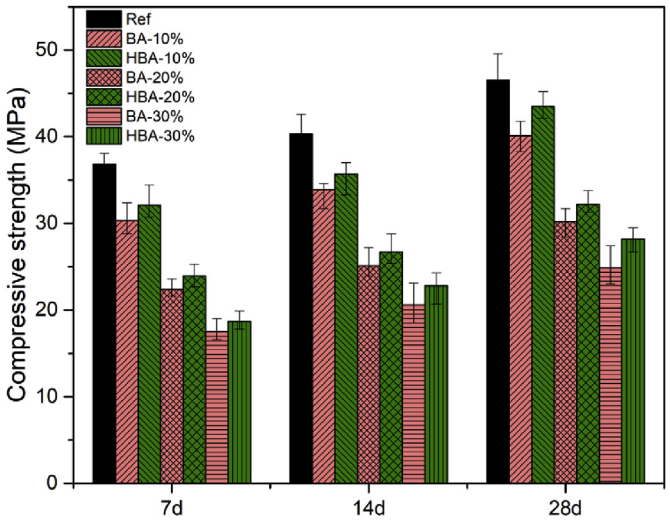

Fig. 7. Compressive strengths of the mortar manufactured with BA and HBA as compared to a reference mortar sample.

30% addition dosage, the water absorption at 28 days is 10.8%. The chloride transport test is performed and the results are shown in Fig. 8(b). The addition of the HBA decreases chloride penetration. The chloride penetration depth of the reference sample is 37.5 mm at 70 days. With 30% addition of HBA, it decreases to 13.2 mm, which has reduced by 65% while the mortar with 30% BA is 55.9 mm. The increase of the water absorption and chloride penetration depth can be attributed to the porous structure of the bottom ash, which increases the ITZ in the mortar matrix, which results in more channels for water transport. This phenomenon is particularly important for applications of BA in cementitious materials, especially in the marine environment. As concrete structures are always unsaturated, capillary absorption largely controlled the ingress of water. The addition of the hydrophobic bottom ash can build a hydrophobic barrier against water penetration.

3.3. Environmental impact assessment

The application of the MSWI bottom ash is restricted by the presence of heavy metals and the anions (i.e., chlorides and sulfates). The contents of these contaminants are regulated by the Dutch legislation (Soil Quality Decree, 2013). In Table 4. The leaching of the contaminants from original BA, HBA and the mortars containing HBA is given. Moreover, to assess the influence of the modification process on the washing of contaminants from BA, a reference sample was made and its leaching was assessed. The reference sample of BA went through same modification process in the absence of the functionalizing agent, i.e., stearic acid. For the original BA, the leaching of the Cr, Cu, Mo, Sb, Cl, and SO_4^{2-} was found to be above the permissible limits. The high leachable content of these contaminants in the BA limits its use as a building material.

The modification process of the BA contributes in reducing the leaching of contaminants decreased significantly, the most significant decrease was noted in the content of Cu, Cl and SO_4^{2-} by 82%, 97% and 56%, respectively. After the functionalization process, HBA shows a further decrease in the leaching of the major contaminants with exception to Sb and sulfates. The leaching of the HBA increases for these elements as compared to the original sample of bottom ash. The increased leaching of Sb and sulfates indicates that modification process can affect the mineral phases that were responsible for the immobilization of these contaminants. The

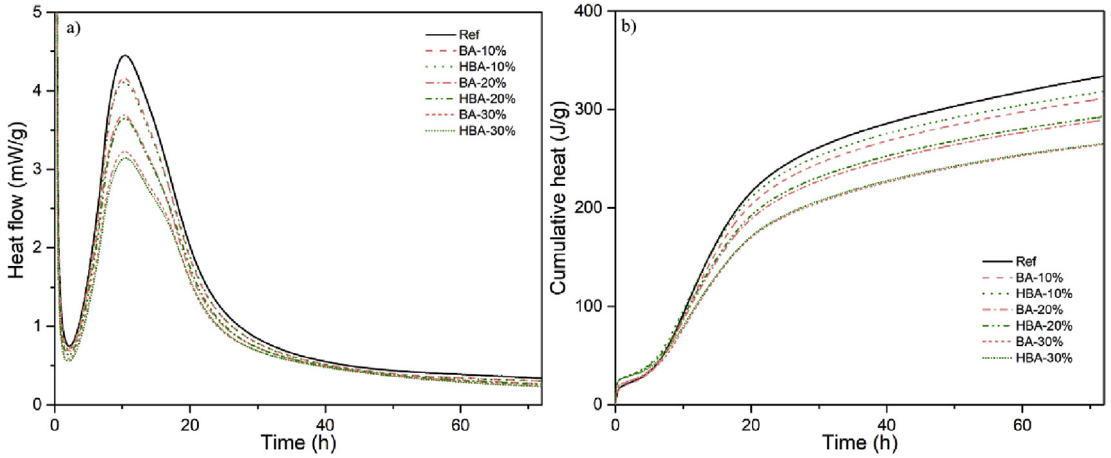

Fig. 6. Normalized heat flow (a) and cumulative heat of hydration (b) of the mixes with different contents of BA and HBA.

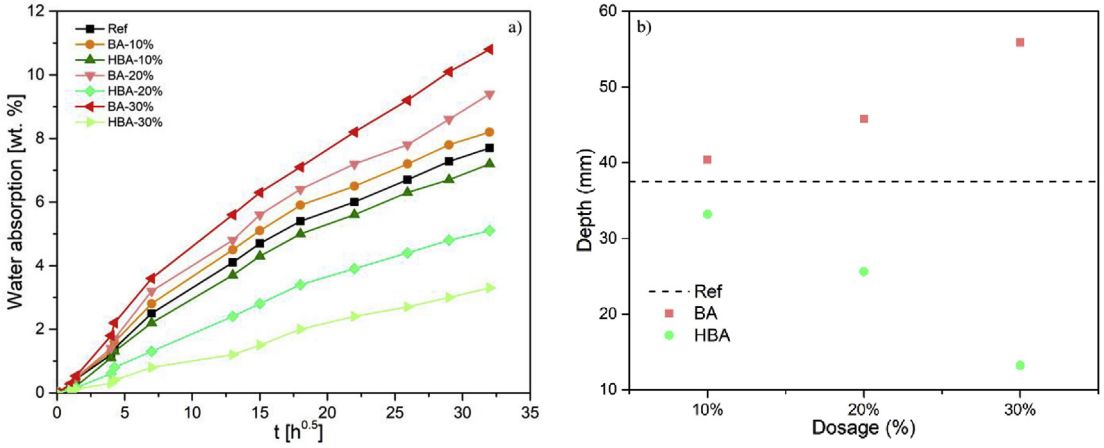

Fig. 8. a) Water absorption test of the mortars; b) chloride penetration depth of the mortars.

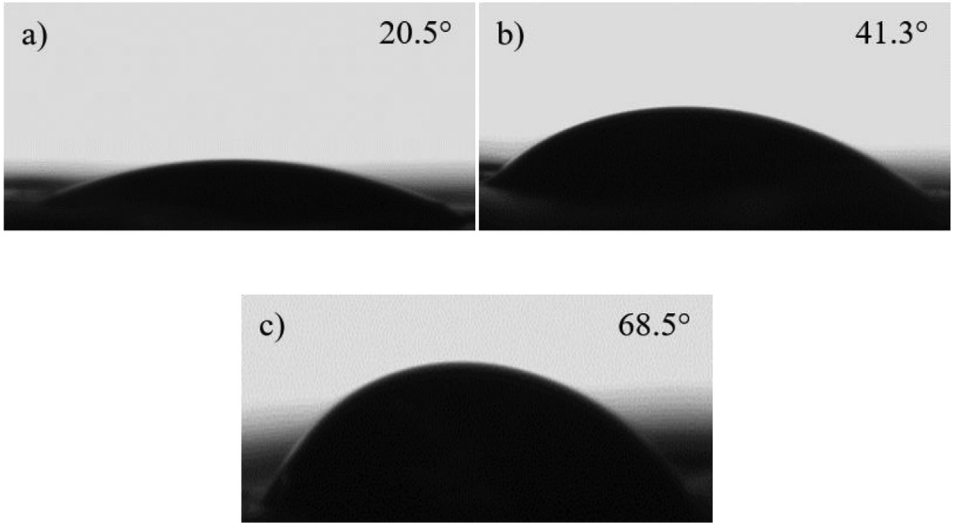

Fig. 9. The water contact angle of the hybrid mortars: a) with 10% replacement, b) with 20% replacement, c) with 30% replacement.

Table 4
Determined concentrations of contaminants (mg/kg) after leaching tests of functionalized samples and reference samples, and their allowed emission limits regulated by the soil quality decree.

	Granular material Legal limits[a]	BA	Reference[b]	HBA	30% BA mortar	30% HBA mortar
Ba	22.00	0.51	0.81	0.72	0.12	<0.05
Cr	0.63	1.14	0.67	0.77	0.09	0.05
Cu	0.90	6.53	1.96	1.16	0.17	<0.2
Mo	1.00	1.20	0.52	0.70	0.22	0.20
Sb	0.32	0.91	0.74	1.22	0.22	0.22
As	0.90	0.16	0.19	0.19	0.21	0.22
Cd	0.04	L.D.	L.D.	L.D.	L.D.	L.D.
Co	0.54	0.05	0.05	0.05	<0.22	<0.22
Pb	2.30	L.D.	L.D.	L.D.	<0.30	<0.30
Ni	0.44	0.07	0.05	0.05	<0.27	<0.28
Se	0.15	0.45	0.41	0.37	0.32	0.33
Sn	0.40	L.D.	L.D.	L.D.	L.D.	L.D.
V	1.80	0.12	0.14	0.12	0.30	0.29
Zn	4.50	0.52	0.63	0.74	0.23	<0.10
Cl	616	11,367	323	367	650	60
SO_4^{2-}	2430	20,979	7703	9161	450	80

[a] The legal limits established by the Dutch soil quality decree for the use of granular material in the open environment without any insulation.
[b] The reference sample of BA was prepared in the same manner as HBA but in the absence of stearic acid to assess the influence of the functionalization process on the leaching properties.

leaching of the heavy metals and anions from the material that shows hydrophobic properties indicate towards the very heterogeneous surface properties of the ash residue. The functionalization of these particles is only possible on the surface, which provides reactive sites for the reaction with stearic acid. The rest of the surface will remain unmodified that would interact with water during leaching test and leads to the leaching of the contaminants. The leaching of the mortars containing 30% of the original BA and modified HBA is given in Table 3 as well; both kind of samples shows leaching below the limits. The leaching of the mortar, which had modified BA, was much lower than the mortar containing original bottom ash. The decrease in the leaching of the contaminants can also be attributed to the dilution of HBA by the cementitious matrix.

4. Conclusions

In this study, a wet chemistry method is applied to prepare hydrophobic bottom ash with stearic acid as a modifying agent. The influences of the bottom ash on the hydration of the cement, compressive strength, capillary water absorption and long-term chloride diffusion of the mortars are investigated. The optimum SA concentration was characterized to be 4%, showing hydrophobic properties of the powder with a contact angle of 141°. The application of the HBA significantly improved the transport property of the mortar. With 30% addition of HBA, the capillary water absorption rate and chloride penetration depth are decreased by 57% and 65%, as compared to the reference sample. The functionalization of the bottom ash particle reduces the leaching of the chlorides, sulfates, copper and molybdenum by 97%, 56%, 82% and 42%, respectively. Moreover, the mortars containing 30 wt% of HBA shows improved leaching properties, because of the dilution effect and immobilization potential of the cementitious matrices.

Declaration of competing interest

The authors certify that they have no conflicts of interest nor affiliations in any organization or entity with any financial interest, or non-financial interest in the subject matter or materials discussed in this manuscript.

Acknowledgements

The authors would like to acknowledge the financial support by NWO foundation (Project number 10019729: “Environmental concrete based on the treated MSWI bottom ashes”) and the EPSRC-NSFC Joint Research Project (No. 51461135005) for funding this research. Mrs. A.C.A. Delsing in the lab of Building Physics and Services at Eindhoven University of Technology is acknowledged for providing experimental support on the SEM analysis. Furthermore, the authors wish to express their gratitude to the following sponsors of the Building Materials research group at TU Eindhoven: Rijkswaterstaat Grote Projecten en Onderhoud; Graniet-Import Benelux; Kijlstra Betonmortel; Struyk Verwo; Attero; Enci; Rijkswaterstaat Zee en Delta-District Noord; Van Gansewinkel Minerals; BTE; V.d. Bosch Beton; Selor; GMB; Icopal; BN International; Eltomation; Knuaf Gips; Hess AAC Systems; Kronos; Joma; CRH Europe Sustainable Concrete Centre; Cement & Beton Centrum; Heros; Inashco; Keim; Sirius International; Boskalis; NNERGY; Millvision; Sappi and Studio Roex (in chronological order of joining).

Appendix A. Supplementary data

Supplementary data to this article can be found online at https://doi.org/10.1016/j.jclepro.2019.119341.

References

Alam, Q., Florea, M.V.A., Schollbach, K., Brouwers, H.J.H., 2017. A two-stage treatment for Municipal Solid Waste Incineration (MSWI) bottom ash to remove agglomerated fine particles and leachable contaminants. Waste Manag. 67, 181–192. https://doi.org/10.1016/J.WASMAN.2017.05.029.

Alam, Q., Hendrix, Y., Thijs, L., Lazaro, A., Schollbach, K., Brouwers, H.J.H., 2019a. Novel low temperature synthesis of sodium silicate and ordered mesoporous silica from incineration bottom ash. J. Clean. Prod. 211, 874–883. https://doi.org/10.1016/j.jclepro.2018.11.173.

Alam, Q., Lazaro, A., Schollbach, K., Brouwers, H.J.H., 2020. Chemical speciation, distribution and leaching behavior of chlorides from municipal solid waste incineration bottom ash. Chemosphere 241, 124985. https://doi.org/10.1016/J.CHEMOSPHERE.2019.124985.

Alam, Q., Schollbach, K., Rijnders, M., van Hoek, C., van der Laan, S., Brouwers, H.J.H., 2019b. The immobilization of potentially toxic elements due to incineration and weathering of bottom ash fines. J. Hazard Mater. 379, 120798. https://doi.org/10.1016/J.JHAZMAT.2019.120798.

Alam, Q., Schollbach, K., van Hoek, C., van der Laan, S., de Wolf, T., Brouwers, H.J.H., 2019c. In-depth mineralogical quantification of MSWI bottom ash phases and their association with potentially toxic elements. Waste Manag. 87, 1–12. https://doi.org/10.1016/j.wasman.2019.01.031.

Arbatan, T., Fang, X., Shen, W., 2011. Superhydrophobic and oleophilic calcium carbonate powder as a selective oil sorbent with potential use in oil spill clean-ups. Chem. Eng. J. 166, 787–791.

Bolokang, A.S., Motaung, D.E., Arendse, C.J., Muller, T.F.G., 2015. Formation of the metastable FCC phase by ball milling and annealing of titanium–stearic acid powder. Adv. Powder Technol. 26, 632–639.

Build, N.T., 1995. 443. Concrete, Hardened: Accelerated Chloride Penetration. method, Nord.

Caprai, V., Florea, M.V.A., Brouwers, H.J.H., 2018a. Evaluation of the influence of mechanical activation on physical and chemical properties of municipal solid waste incineration sludge. J. Environ. Manag. 216, 133–144. https://doi.org/10.1016/J.JENVMAN.2017.05.024.

Caprai, V., Schollbach, K., Brouwers, H.J.H., 2018b. Influence of hydrothermal treatment on the mechanical and environmental performances of mortars including MSWI bottom ash. Waste Manag. 78, 639–648. https://doi.org/10.1016/J.WASMAN.2018.06.030.

Carvalho, S.Z., Vernilli, F., Almeida, B., Oliveira, M.D., Silva, S.N., 2018. Reducing environmental impacts: the use of basic oxygen furnace slag in portland cement. J. Clean. Prod. 172, 385–390.

De Vries, J., Polder, R.B., 1997. Hydrophobic treatment of concrete. Constr. Build. Mater. 11, 259–265.

Du, H., Du, S., Liu, X., 2015. Effect of nano-silica on the mechanical and transport properties of lightweight concrete. Constr. Build. Mater. 82, 114–122.

Elfmarkova, V., Spiesz, P., Brouwers, H.J.H., 2015. Determination of the chloride diffusion coefficient in blended cement mortars. Cement Concr. Res. 78, 190–199.

EN, T.S., 2005. 196-1. Methods of testing cement–Part 1: determination of strength. Eur. Comm. Stand. 26.

Feng, L., Li, S., Li, Y., Li, H., Zhang, L., Zhai, J., Song, Y., Liu, B., Jiang, L., Zhu, D., 2002. Super-hydrophobic surfaces: from natural to artificial. Adv. Mater. 14, 1857–1860.

Feng, Y., Chen, S., Cheng, Y.F., 2018. Stearic acid modified zinc nano-coatings with superhydrophobicity and enhanced antifouling performance. Surf. Coat. Technol. 340, 55–65.

Gao, X., Yuan, B., Yu, Q.L., Brouwers, H.J.H., 2017. Characterization and application of municipal solid waste incineration (MSWI) bottom ash and waste granite powder in alkali activated slag. J. Clean. Prod. 164, 410–419. https://doi.org/10.1016/J.JCLEPRO.2017.06.218.

Ghafari, E., Arezoumandi, M., Costa, H., Júlio, E., 2015. Influence of nano-silica addition on durability of UHPC. Constr. Build. Mater. 94, 181–188.

Greendeal-GD076, 2012. Greendeals GD076: sustainable useful application of WtE bottom ash [WWW document] Dutch Minist. Infrastruct. Environ. Times.

Hossain, M.M., Karim, M.R., Hasan, M., Hossain, M.K., Zain, M.F.M., 2016. Durability of mortar and concrete made up of pozzolans as a partial replacement of cement: a review. Constr. Build. Mater. 116, 128–140.

Hu, Z., Zen, X., Gong, J., Deng, Y., 2009. Water resistance improvement of paper by superhydrophobic modification with microsized CaCO3 and fatty acid coating. Colloid. Surf. Physicochem. Eng. Asp. 351, 65–70.

Jiang, L., Zhao, Y., Zhai, J., 2004. A lotus-leaf-like superhydrophobic surface: a porous microsphere/nanofiber composite film prepared by electrohydrodynamics. Angew. Chem. 116, 4438–4441.

Kalla, P., Rana, A., Chad, Y.B., Misra, A., Csetenyi, L., 2015. Durability studies on concrete containing wollastonite. J. Clean. Prod. 87, 726–734.

Liu, Z., Hansen, W., 2016. Effect of hydrophobic surface treatment on freeze-thaw durability of concrete. Cement Concr. Compos. 69, 49–60.

Pham, V.H., Dickerson, J.H., 2014. Superhydrophobic silanized melamine sponges as high efficiency oil absorbent materials. ACS Appl. Mater. Interfaces 6, 14181–14188.

Qu, Z.Y., Yu, Q.L., 2018. Synthesizing super-hydrophobic ground granulated blast furnace slag to enhance the transport property of lightweight aggregate concrete. Constr. Build. Mater. 191, 176–186.

Qu, Z.Y., Yu, Q.L., Brouwers, H.J.H., 2018. Relationship between the particle size and

dosage of LDHs and concrete resistance against chloride ingress. Cement Concr. Res.
Sanchez, F., Sobolev, K., 2010. Nanotechnology in concrete—a review. Constr. Build. Mater. 24, 2060–2071.
Shi, Y., Jiang, R., Liu, M., Fu, L., Zeng, G., Wan, Q., Mao, L., Deng, F., Zhang, X., Wei, Y., 2017. Facile synthesis of polymeric fluorescent organic nanoparticles based on the self-polymerization of dopamine for biological imaging. Mater. Sci. Eng. C 77, 972–977.
Silva, R.V., de Brito, J., Lynn, C.J., Dhir, R.K., 2017. Use of municipal solid waste incineration bottom ashes in alkali-activated materials, ceramics and granular applications: a review. Waste Manag. 68, 207–220. https://doi.org/10.1016/j.wasman.2017.06.043.
Soil Quality Decree, 2013. Ministerie van Volkshuisvesting, Ruimtelijke Ordeling en Milieubeheer. Regeling Bodemkwaliteit, VROM, Den Haag: Ruimte en Milieu. Ministerie van Volkshuisvesting, Ruimtelijke Ordeling en Milieubeheer.
Spathi, C., Young, N., Heng, J.Y.Y., Vandeperre, L.J.M., Cheeseman, C.R., 2015. A simple method for preparing super-hydrophobic powder from paper sludge ash. Mater. Lett. 142, 80–83. https://doi.org/10.1016/j.matlet.2014.11.123.
Supit, S.W.M., Shaikh, F.U.A., 2015. Durability properties of high volume fly ash concrete containing nano-silica. Mater. Struct. 48, 2431–2445.
Van Tittelboom, K., De Belie, N., De Muynck, W., Verstraete, W., 2010. Use of bacteria to repair cracks in concrete. Cement Concr. Res. 40, 157–166.
Wong, H.S., Barakat, R., Alhilali, A., Saleh, M., Cheeseman, C.R., 2015. Hydrophobic concrete using waste paper sludge ash. Cement Concr. Res. 70, 9–20. https://doi.org/10.1016/J.CEMCONRES.2015.01.005.
Yang, J., Wang, F., He, X., Su, Y., 2018. Pore structure of affected zone around saturated and large superabsorbent polymers in cement paste. Cement Concr. Compos.
Zhang, X., Huang, Q., Deng, F., Huang, H., Wan, Q., Liu, M., Wei, Y., 2017. Mussel-inspired fabrication of functional materials and their environmental applications: progress and prospects. Appl. Mater. Today 7, 222–238.
Zhang, Y., Zhang, M., Ye, G., 2018. Influence of moisture condition on chloride diffusion in partially saturated ordinary Portland cement mortar. Mater. Struct. 51, 36.